

APPLICATION OF MÖSSBAUER BACKSCATTERING GEOMETRY
IN INDUSTRY¹

J. Lipka² I. Tóth, M. Prejsa, R. Gröne
Department of Nuclear Physics and Technology, Slovak Technical University,
Ilkovicova 3, 812 19 Bratislava, Slovakia

Received 28 September 1994, in final form 10 October 1994, accepted 7 November 1994

A description of the scattering experiment and analysis of the Mössbauer spectra form the first part of this contribution. A comparison of reflection and transmission spectra shows that the lines in reflection geometry are broadened considerably (20 %) due to thickness distortion. In the second part we present the results we have obtained using this geometry in the study of corrosion products from nuclear power plants, transformer sheets and so called Mars samples analogues.

INTRODUCTION

In general, Mössbauer spectroscopy can be performed either in the transmission mode (TMS) or in backscattering mode by detecting the decay products of the de-excitation of the nuclei in the specimen which have been resonantly excited by the source radiation. In the latter case, one can use conversion electron Mössbauer spectroscopy (CEMS), conversion X-ray Mössbauer spectroscopy (CXMS) or re-emitted γ -ray Mössbauer spectroscopy (RGMS).

A summary of major events during decay of the excited ($I=3/2$) state of ^{57}Fe is given in Table 1, [1]. A number of backscattering studies have been published so far mainly for investigating surface properties. Because of the high internal conversion coefficient, most reflection Mössbauer spectroscopy studies have used the X-rays and electrons associated with internal conversion rather than the resonantly scattered γ -rays which have larger depths range in solids. Because of the possibility to investigate selectively the material at different depths, Mössbauer scattering experiments often yield information that cannot be obtained in the standard transmission geometry, but they are also more complex both experimentally and conceptually, and they must be carefully adapted to the specific problem to be studied. The additional conditions e.g. thickness distortion, the effect of rescattering, the total attenuation coefficient consisting of both resonant

¹ Presented at the Colloquium on Mössbauer Spectroscopy in Material Science, Kočoverce, Slovakia, October 3-6, 1994

²E-mail address: Lipka@elf.stuba.sk

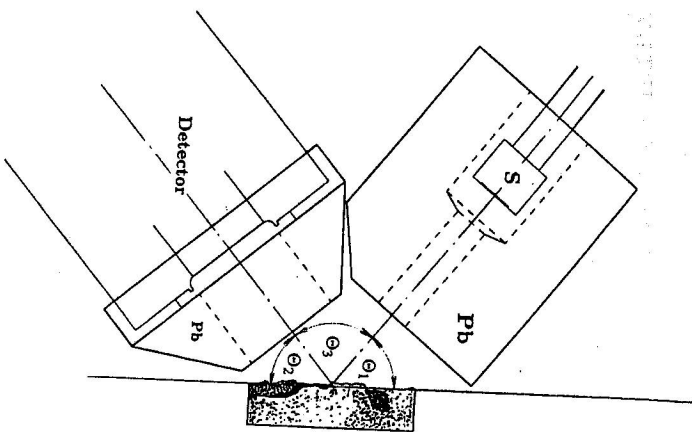


Fig. 1. Diagram of the experimental geometry. S is the source. The sample has both a polished and an unpolished (rough) surface ($\Theta_1 = \Theta_2 = 50^\circ$ and $\Theta_3 = 80^\circ$).

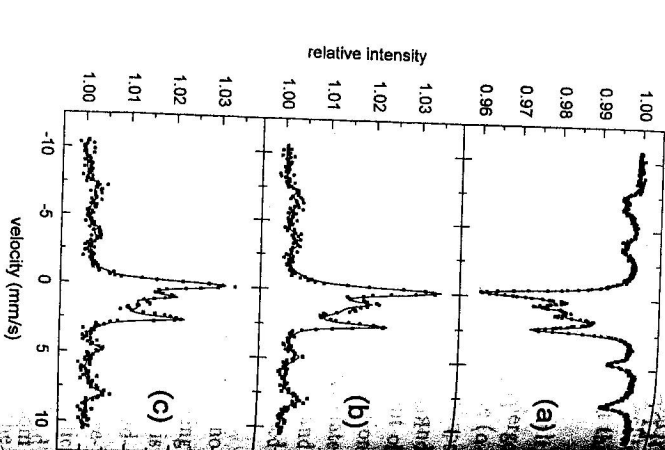


Fig. 2. Mössbauer spectra of a basalt obtained in transmission (a) and backscattering geometries from polished (b) and unpolished (c) sides.

and non-resonant γ -radiation and interference effect between Rayleigh, Compton and Mössbauer scattering should be taken into account [2]. However in practice the situation is simplified since some of the effects have no substantial influence on Mössbauer spectra obtained from polycrystalline samples. For example the interference term from the nuclear resonant and coherent Rayleigh scattering processes at a scattering angle of 90° is negligible [3]. The thickness distortion usually must be accounted for when quantitative information is to be extracted from a backscatter spectrum because of the thickness distortion will be only negligible when $f n_A \sigma_A(E) \ll \mu$ (where $f n_A$ is the recoil free fraction of the absorber, n_A is the number of ^{57}Fe atoms per cm^3 , σ_A is the scattering cross section and μ is the non-resonant mass attenuation coefficient), i. e. when Fe is the dominant heavy atom in the material under investigation [4].

EXPERIMENTAL AND DISCUSSION

We have studied several kinds of samples including basaltic rocks and impactites.

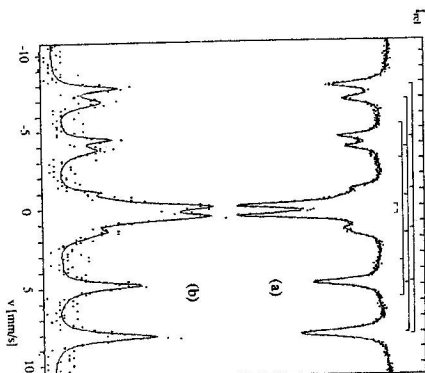


Fig. 3. Mössbauer spectra of the sample from the primary circuit of the water-cooled reactor measured in transmission (a) and by scattering modes (b).

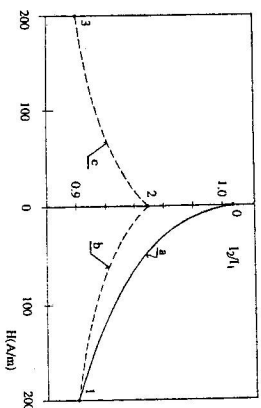


Fig. 4. I_2/I_1 versus magnetic field H applied at an angle $\alpha = 45^\circ$ with respect to the rolling direction.

All samples were measured using both scattering and transmission geometry. The arrangement of the apparatus for backscattering spectroscopy is illustrated in Fig. 1. A scintillation detector with a NaI crystal was used as counter. The angle Θ_1 between the plane of the sample and direction of propagation of γ -rays and Θ_2 that defined by the sample plane and orientation of the detector, were both equal to 50° . Backscattered spectra were recorded in 256 channels of the multichannel analyzer. The ^{57}Co in Cr source was used. Average counting time was 200 hrs. All the basalt samples were

Table 1. Energies, relative probabilities and penetration depths of photons and electrons emitted after resonant excitation of the 14.4 keV state of ^{57}Fe . Adapted from [1].

^{57}Fe	Energy (keV)	per 100 absorption events	Depth range in typical iron based solids (nm)
γ photons	14.4	9	20,000-40,000
K X-rays	6.4	27	10,000-20,000
L X-rays	0.7	0.002	
K conversion electrons	7.3	81	10-400
L conversion electrons	13.6	9	20-1300
M conversion electrons	14.3	1	20-1500
KLL Auger electrons	5.4	63	7-200
LMM Auger electrons	0.53	60	1-2

Table 2. Relative areas of the subspectra (in %) and average linewidths (Γ) of the 5 components; $M = M_1 + M_2$ (two magnetic components); Δ_i represent doublets, Γ_{aver} (mm/s) is calculated as a simple mean of the line widths of the 5 spectral components.

Sample	M	Δ_1	Δ_2	Δ_3	Γ_{aver}
Transmission	32	27	28	11	0.56
Scat. - rough	26	26	30	16	0.65
Scat. - polished	28	26	26	18	0.67

measured on two sides; one has a polished flat surface resulting from a mechanical polishing and the other side has roughness profiles with a topographic depth up to 4 mm. Powdered material for transmission Mössbauer spectroscopy was produced by grinding of the bulk sample. TM spectra were measured with the same spectrometer using the same detector and source in 512 channels. The average counting time was 7 hrs. The spectra were fitted with five components: two sextet (M) and three doublet (Δ).

Typical transmission and corresponding reflection spectra are shown in Fig. 2. Comparison of TM spectra with RGM spectra of the same specimens reveals some differences. For example in Fig. 2 we see a relatively large difference in the relative area of the line at about 1.4 mm s^{-1} and in the case of an impactive sample (not shown) a magnetic component present in TM spectrum is absent in the backscattering spectrum. We attribute these differences to the different states of the sample. There is also the possibility that changes (e.g. oxidation state) could be introduced by weathering as well as in the process of polishing.

The line widths are systematically found to be larger when samples are measured in scattering geometry. The γ -ray beams in both measuring modes are well collimated, so that cosine broadening is estimated to be below 2% and we observe increases of line widths up to 20% (see Table 2). The relative contribution of the coherent Rayleigh

scattering effect has been estimated using an average atomic number of the samples equal to 10. One then calculates that the intensity of Mössbauer scattering dominates that of Rayleigh scattering by a factor of 120. So we attribute the remaining line broadening to thickness distortion in the scattering experiment. An apparent effect of roughness can be observed in the scattering spectra from the rough and polished surfaces as differences in the relative areas of the subspectra. These differences, we believe, are, in fact, not mainly caused by roughness, but by the different states of the sample.

INDUSTRIAL APPLICATIONS

The variability of the properties and the composition of the corrosion products of the stainless CrNi and mild steels in dependence on the conditions (temperature, acidity, etc.) in the primary circuit of the nuclear power plant is of such range that, in practice, it is impossible to determine the properties of the corrosion products for an actual case from the theoretical data only. Since the decontamination processes for the materials of the water-cooled reactor (VVER 440) primary circuit are in the process of the development as well as for the gas-cooled reactor (A1) secondary and auxiliary circuits it is necessary to measure and analysis the real samples taken from both primary and secondary circuits [5]. These samples were investigated by various methods, including Mössbauer spectroscopy. The corrosion layers were separated by scraping of the rust from the surface and powder samples were studied by transmission geometry. When the samples were compact, we have used scattering geometry. For such analysis the piece of the tube was cut in order to have a possibility to measure the inner part. It should be noted that the gamma spectroscopic measurements give no evidence of the presence of low-energy γ radiation emitted from the samples. Typical Mössbauer spectra measured in transmission and scattering modes are shown in Fig. 3. The structure of the observed spectra consists generally of two parts: a six line pattern corresponding to magnetically ordered phases and the central doublet from paramagnetic compounds. The structure and relative area of the components of each pattern vary from sample to sample. The magnetic component corresponds to the cation deficient magnetite (Fig. 3a). In some samples of mild steel haematite and small quantities of goethite and maghemite were identified.

Backscattering geometry was also applied to study the magnetic properties of oriented 3% Si-Fe transformer sheets. The aim of this work was to prove a dependence of the integral intensity ratio of the first two lines (I_2/I_1) of Mössbauer spectra on the magnetic domain orientation.

The samples were prepared in laminated form from polycrystalline commercial grain-oriented 3% Si-Fe material. Measurements of the Mössbauer spectra were performed in DC magnetic field. The magnetic field H was always applied at the same angle α with respect to the rolling axis of the sample.

The influence of an applied magnetic field on the line intensity ratio I_2/I_1 is shown in Fig. 4 for the samples cut at angle $\alpha = 45^\circ$. The measured curve "a" corresponds to the primary magnetization curve, i.e. magnetization from the point 0 up to point 1 in Fig. 4. The ratio I_2/I_1 decreases with increasing magnetic field intensity H . The intensity ratio is constant when the magnetization approaches saturation. When the

magnetization process was turned from the saturation magnetic induction $+B_r$ to the remanent induction $+B_r$, the values of I_2/I_1 did not follow curve "a": the different curve "b" was measured for this part of the hysteresis loop. For the values of the applied magnetic field in the opposite direction, I_2/I_1 is plotted as curve "c", which is symmetrical to curve "b". When the magnetization is changed from the saturated induction in opposite direction, $-B_m$, to the remanent state, $-B_r$, the dependence of I_2/I_1 on H is in fair agreement with the curve "c". A similar situation exists for the process on the rest of the hysteresis loop because the measured values of I_2/I_1 corresponded to curve "b". No hysteresis effect is seen on the curve of I_2/I_1 versus H . It is interesting that curve a corresponding to the cycle from the demagnetized state to the saturation induction and from this state to the remanent induction B_r is displaced.

We attempted to explain the observed effect illustrated in Fig 4 by changes of domain structure during the magnetization. In accordance with the observed grain-surface domain structure, the unambiguity of I_2/I_1 ratios is probably due to changes of supplementary domains which are formed on grain boundaries and in misoriented grains [6]. We believe that this effect is not connected with the changes of the main domain structure of these slabs.

SUMMARY

We can conclude that there are two kinds of difficulties in making truly quantitative phase analysis in scattering geometry: the first is the methodological problems (e.g. the time required to collect a γ -ray scattering spectrum is an order of magnitude longer than that for an absorption spectrum). Secondly, the analysis of spectra obtained in scattering geometry is complicated by specific effects related to scattering. On the other hand our results obtained on the real samples (corrosion products and transformer sheets) confirm the advantage of the scattering geometry for nondestructive analysis without special sample preparation.

REFERENCES

- [1] F. E. Wagner: *J. Phys.* **37** (1976), C6-673;
- [2] V. V. Morosov: *Hyp. Int.* **72** (1992), 343;
- [3] B. Balko, G. R. Hoy: *Phys. Rev.* **B10** (1974), 36;
- [4] B. Fultz, J. W. Morris, Jr.: *Nucl. Instr. Methods* **188** (1981), 197;
- [5] J. Lipka, J. Blazek, D. Majersky, M. Migliorini, M. Seberini, J. Cirak, I. Toth, R. Grone: *Hyp. Int.* **57** (1990), 1969;
- [6] J. Stama, M. Prejsar: *J. Magn. Magn. Mat.* **41** (1984), 35;